16th World Conference on Earthquake, 16WCEE 2017

Santiago Chile, January 9th to 13th 2017

Paper N° 2829 (Abstract ID)

Registration Code: S-X1464698401

ANALYSIS OF DIAPHRAGM SEISMIC DESIGN FORCES IN TWO 5-STORY MINIATURE STEEL FRAME BUILDINGS TESTED IN SHAKING TABLE

J. Blandon-Valencia[(1)], M. Rodriguez[(2)]

[(1)] *Professor Universidad Nacional de Colombia, jjblandon@unal.edu.co*
[(2)] *Professor, Instituto de Ingenieria, Universidad. Nacional Autonoma de Mexico, mrod@servidor.unam.mx*
…

Abstract

The use of precast buildings is important for solving the housing problem in Latin America. Precast buildings are also used for other purposes, such as commercial malls, industrial and office buildings. Precast and prestressed floor systems offer significant advantages in many of the construction phases of a building, among which are: manufacturing time, reduced shoring system and they can be used in combination with any structural system such as concrete, steel or masonry. However, the use of precast structures has not been extensive, mainly due to the limited dissemination on the latest developments regarding the seismic design of diaphragms, lack of unified seismic design procedures and comprehensive regulations for precast floor systems. With cast-in-place reinforced concrete buildings there are also cases where the floor system would need especial detailing to resist seismic actions, such as for example floor systems with openings for elevators or stairs. Although every building has a type of floor system, little attention had been given to the criteria for evaluating and resisting in-plane diaphragm forces. However, that changed as a result of the 1994 Northridge earthquake in California. The collapses of some precast structures in this earthquake suggested that they were due to floor system failures. Most of these cases were parking buildings with a structural system based on the combination of perimetrical seismic resisting reinforced concrete walls, and precast concrete frames, primarily designed to resist gravity loads. This research presents the results of analytical and experimental studies of two miniature 5-story steel buildings tested on the shaking table of the National University of Mexico in order to review the seismic behavior of rigid floor systems in buildings, considering the effect of in-plane diaphragm forces. The results of shaking table tests are compared with results from inelastic analysis as well as with those using code provisions. This paper reviews different procedures for the analysis of diaphragm seismic design forces. A procedure for defining in-plane floor forces for use in design of building diaphragms is proposed in this study. Results using this procedure showed acceptable agreement with measured inertial forces.

Keywords: Diaphragm, Seismic, Design, Forces, Experimental

1. Introduction

It should be mentioned that in the 1994 Northridge earthquake, the measured inertial horizontal accelerations in some buildings showed floor acceleration amplifications that were greater than those computed using building codes [1]. The collapse of some precast structures in this earthquake suggested that they were due to failure in floor systems [2]. Also, evidences of differences in measured and predicted diaphragm forces were observed in some experimental results of a 5-story precast specimen studied in the PRESS program, which has been described in detail in the literature [3]. The specimen had precast frames in one direction, and in the other direction had concrete walls, and precast post-tensioned concrete frames designed to take only gravity load. The measured lateral forces in the pseudo-dynamic test of the specimen were significantly higher than those calculated with procedures specified by current regulations, suggesting significant higher modes effects [3]. These results suggest that existing procedures specified by building codes for defining in-plane diaphragms forces are unsafe and may need revising.

2. Diaphragms Design Considerations

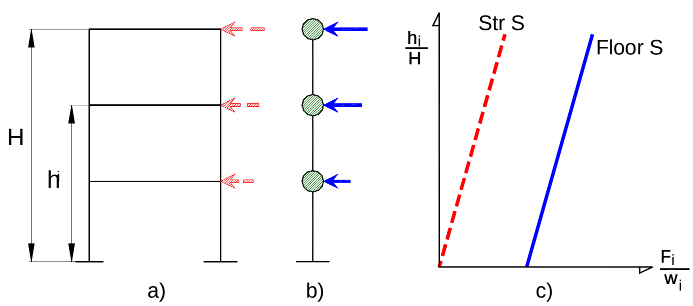

Fig. 1 Structural models for the building design

In earthquake-resistant design of buildings, the primary lateral force resisting system is designed for specified lateral forces. In addition, diaphragm horizontal forces in buildings need to be defined for the seismic design of diaphragms. This process is conceptually explained in Fig. 1, which shows a lateral force resisting system of a building with a height H, and a floor weight w_i, located at a height h_i., Fig. 1b. Fig. 1c shows schematically the horizontal forces distribution in the primary lateral force resisting system, identified as *Str S*, and the diaphragm horizontal forces, identified as *Floor S*. The first set of design forces, represented by a dotted line in Fig. 1(c), are the static analysis forces for the primary lateral force resisting system and it is evaluated using Eq. (1):

$$F_i = \frac{c \cdot W}{R} \cdot \frac{w_i \cdot h_i}{\sum_{j=1}^{n} w_j \cdot h_j} \tag{1}$$

In Eq. (1), c is the elastic coefficient seismic design, W is the total weight of the structure, and R is the response modification factor.

3. Interpretation of Floor Forces Evaluation

3.1 Mexico City Building Code (MCBC) 2004 [4]

In the MCBC the seismic design of diaphragms is part of the code section that defines requirements for the seismic design of nonstructural elements, with no mandatory wording for the seismic design of diaphragms. According to that code section, a nonstructural element is designed assuming that is supported directly on the ground, multiplied by $1+ c'/a_o$, where c' is the factor that multiplies the weight of a nonstructural element, at a given level of a building, to obtain at that level the design force of the lateral force resisting system. Parameter a_o is the PGA defined in the design response spectra.

3.2 ASCE 7-10 Standard. Minimum Design Loads for Buildings and Other Structures [5]

This standard contains provisions for the design of nonstructural components. These provisions are different from those for the design of diaphragms. This standard requires diaphragm forces greater than those specified for the design of the lateral load resisting system, and these forces are required not be less than those determined in accordance with Eq. (2):

$$\frac{F_{px}}{W_{px}} = \frac{\sum_{i=x}^{n} F_i}{\sum_{i=x}^{n} W_i} \tag{2}$$

where F_{px} is the diaphragm design force, F_i is the design force applied in the level i in the earthquake resistant system, w_i is the weight tributary to the level i and w_{px} is the weight tributary to the diaphragm at level x. The lower and upper limit for the values in the Eq. (2) are $0.2 \cdot S_{DS} \cdot I_e$ and $0.4 \cdot S_{DS} \cdot I_e$, respectively, where S_{DS} is the design, 5% damped, spectral response acceleration parameter at short periods, and I_e is the importance factor.

3.3 Rodríguez, Restrepo and Carr proposal [6]

These authors have shown that the computation of in-plane floor forces for design of diaphragms need to consider the effect of higher modes assuming that ductility only affects floor accelerations associated with the first mode of response. The proposed procedure for the computation of in-plane floor forces is summarized in Eq. (4), where the nonlinear response of the lateral load resisting system affects only the first mode, which shows that current seismic design procedures that reduced all modes by the same factor might be unsafe [6].

$$\frac{F_n}{W_n} = \cdot\sqrt{\left[\frac{\Gamma_1 \cdot \phi_n^1 \cdot S_a(T_1, \xi_1)}{g \cdot R_M}\right]^2 + \sum_{i=2}^{n}\left[\Gamma_i \cdot \phi_n^i \cdot \frac{S_a(T_i, \xi_i)}{g}\right]^2} \tag{4}$$

In Eq. (4) F_n is the inertial force at the roof level, n, with a floor weight W_n, Γ_i is the participation factor for the i mode, the $S_a(T_i, \xi_i)$ parameter is the ordinate response spectrum of accelerations for period T_i, and the parameters ξ_i, and ϕ_n^i are the fraction of critical damping and the value of the mode shape i at the level n, respectively. Similarly, the reduction factor, R_M, which takes into account the inelastic behavior of the building, can be assumed equal to the ratio between the maximum overturning moment at the base of a building when responding to a ground motion in the linear elastic range and the maximum overturning moment on the basis for the case of inelastic response for the same ground motion. These overturning moments are obtained as the sum of the moments about the base of the inertial forces F_i.

Based on the results obtained using Eq. (4), Rodriguez, Restrepo and Carr [6] have proposed a simplified version of Eq. (4) for the computation of horizontal absolute accelerations in building levels. The simplified expression defines the maximum acceleration, a_n, at the last level, n, of the building, as:

$$a_n = \frac{F_n}{W_n} = \sqrt{\left[\frac{\eta_1 \cdot S_a(T_1, \xi)}{g \cdot R_M}\right]^2 + \eta_2 \cdot \ln(n) \cdot a_0^2} \tag{5}$$

where a_o is the value of the ordinate corresponding to the design response spectrum at $T=0$, the parameter η_1 takes into account the contribution of the first mode, and η_2 takes into account the contribution of higher modes. The upper bound of Eq. (5) can be obtained with parameters $\eta_1=8/5$ and $\eta_2=1.75$. A lower bound of Eq. (5) is obtained with parameters η_1 and η_2, equal to 6/5 and 5/8, respectively, [7].

Based on Eq. (5), for the design of diaphragms in buildings in Mexico City, the MCBC (2016) draft requires the use of Eq. (6) to define the in-plane floor accelerations at the roof level, a_n:

$$a_n = \frac{F_n}{W_n} = \sqrt{\left[\frac{\eta_1 \cdot a}{R}\right]^2 + \eta_3 \cdot a_0^2} \tag{6}$$

where a is the ordinate of the elastic design response spectrum. Rodriguez and Restrepo [8] have suggested an upper limit of Eq. (6) using $\eta_1=8/5$ and $\eta_3 = 1.4 \cdot \sqrt{n-1} \quad \leq 5$. It should be noted that η_3 in Eq. (6) replaces the parameter $\eta_2\ ln(n)$ in Eq. (5). To obtain the value of the accelerations for levels other than the roof level, the amplification factors, Ω_i and Ω_n, are defined. These factors correspond to the amplification of the accelerations at level i and level n, respectively, that is:

$$\Omega_i = \frac{F_i}{W_i \cdot a_0} \quad \text{and} \quad \Omega_n = \frac{F_n}{W_n \cdot a_0} \tag{7}$$

For an approximate evaluation of the amplification factor Ω_i, in [8] Rodriguez and Restrepo proposed a linear variation from the ground level to the roof level:

$$\Omega_i = 1 + \frac{h_i}{H}(\Omega_n - 1) \tag{8}$$

Once the amplification factor is obtained, Eq. (9) is used to define the in-plane floor forces for the design of building diaphragms:

$$\frac{F_i}{W_i} = \frac{\Omega_i \cdot a_0}{R_s} \tag{9}$$

Where F_i is the inertial force in the diaphragm level, i, of the building with floor weight equal to W_i, and R_s is the reduction factor in the diaphragm due to overstrength and inelasticity, and needs to be specified by a Standard for each type of floor system, and it has values between 1 and 2.

3.4 ASCE 7-2017 Standard. Minimum Design Loads for Buildings and Other Structures [9]

The draft of this Standard has adopted the proposal made in [6] for the computation of floor acceleration at the roof level, C_{pn}, considering the effects of inelastic behavior only in the first mode, and is computed as:

$$C_{pn} = \sqrt{(\Gamma_{m1} \cdot \Omega_0 \cdot C_s)^2 + (\Gamma_{m2} \cdot C_{s2})^2} \tag{10}$$

where Γ_{m1} and Γ_{m2}, are the contribution factors for the first mode and higher modes, respectively, C_{s2} is the seismic coefficient for the higher modes, Ω_0 is the overstrength factor, C_s is the value of the diaphragm design acceleration coefficient for the first mode, and is calculated as $C_s = S_{DS} / (R/I_e)$. The general equation for the distribution of forces through the building height is:

$$\frac{F_{px}}{W_{px}} = \frac{C_{px}}{R_s} \tag{11}$$

where R_s is the reduction factor of diaphragms forces specified in the standard for each type of diaphragm, C_{px} is the diaphragm design acceleration coefficient at Level x, C_{P0} is is the diaphragm design acceleration coefficient at the structure base, and C_{pn} is the diaphragm design acceleration coefficient at the top of the structure. Based on the number of levels, it standard considers two types of distributions. For structures of three or more levels, C_{px} is equals to C_{P0} up to the height equal to $0.8H$, and C_{px} can be interpolated linearly between C_{P0} and C_{pn} from $0.8H$ and H. For structures up to two levels, C_{px} is linearly interpolated between C_{P0} and C_{px} throughout the height H.

4. Study of the Inertial Forces in Miniature Buildings Tested in Shaking Table

4.1 Specimens description

The test specimens studied in this research were conceived as “miniature” 5-story buildings, therefore, when testing these specimens in the shaking table tests, it was not necessary to scale the intended input ground motion. These test specimens followed detailing of a similar specimen that was tested before at the University of Canterbury in New Zealand [10].

The lateral load resisting system of the test specimens in the transverse direction, also loading direction in the shaking tests, consisted of one-bay moment resisting steel frames, and they are shown in Fig. 2 at axes 1 and 2. One-way steel planks spanning between the longitudinal frames and beams were used as floor units, see Fig. 2, [11]. Each set of planks in a span was bolted to a 3/16” thick top steel plate to explicitly ensure diaphragm action by transferring floor inertial forces by arching, see Fig. 2a. [10].

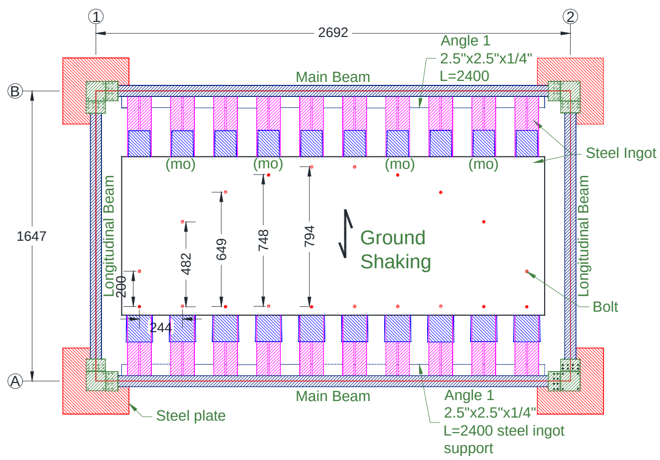

a) EM1 and EM2 typical floor plan

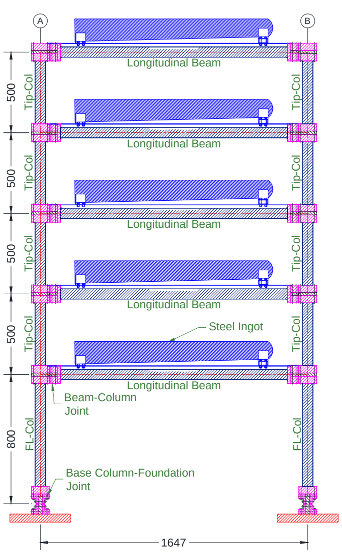

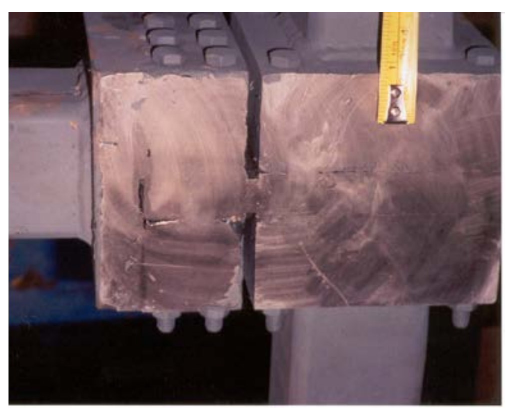

b) Side elevation c) Detail typical beam-column connection

Fig. 2 General details of the tested buildings, with dimensions in millimeters

The test unit identified as *EM1* corresponds to the building tested with 10 steel planks and ingots per level. The building identified as *EM2* had 60% of the mass of the *EM1* building. Test unit EM2 was constructed eliminating four steel planks per level, which are identified as *(mo)* in Fig.2a. The test units represented frame buildings, in which the inelastic behavior was concentrated in elements called fuses. After testing, only the fuses are replaced and a new test can be done quickly, saving considerably time and material. Fig. 2b is a lateral elevation of the frame buildings showing the location of fuses. Fig. 2c shows the detail of these elements and the slotted flat bars used to concentrate the inelastic actions.

The design considered that the test units were located on the coast of Acapulco, in Guerrero State, assuming the strong column-weak beam mechanism. The structural analysis was carried out considering that the resistance of the connections among the different elements was due only to the fuses. Elastic seismic design coefficients, c, were 0.36 and 0.86 for the *EM1* and *EM2* buildings, respectively. The seismic behavior factor, Q, was considered equal to 4 in the two buildings and the drift limit was set to 0.012.

4.2 Materials

It was necessary to know the mechanical properties of the fuses' material, and tension tests of the fuses were performed. Fig. 3a shows the stress-strain plot for the *EM1* building fuses and Fig. 3b shows the curve for the steel in the *EM2* building fuses. The latter figure shown two kinds of curves obtained for different rates of loading. The curve identified as *Slow* was obtained when the load was applied at a rate of 5.8 kN/min, and the curve identified as *Fast* when the load was applied at a rate of 118 kN/min. For the building *EM1* was applied only one rate of load of 11.8 kN/min. These tests were performed to determine the effect of the rate of loading in the material response. Fig. 3 shows the values for the yield stress, f_y, and maximum stress, f_{SU}. Values for yielding strain, ε_y, and ultimate strain, ε_u are also shown. Beams and columns were made of square hollow steel sections 64mmx64mmx 4.83m, with a nominal yield stress, f_y, 350 MPa.

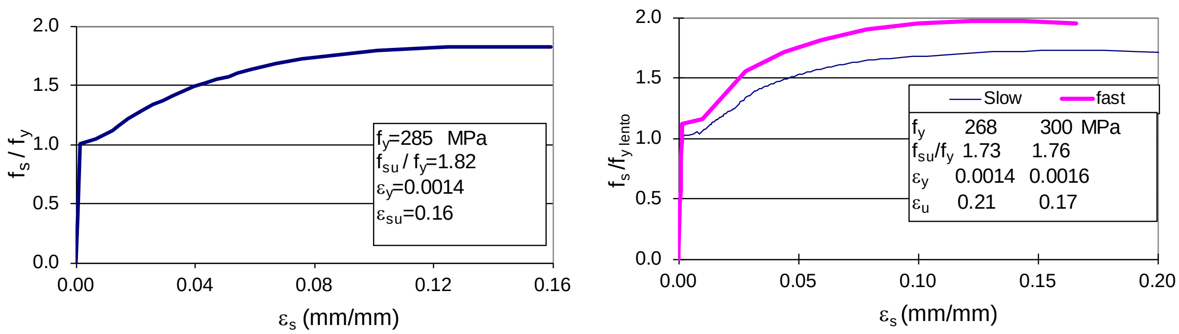

a) Building EM1 b) Building EM2

Fig. 3. Mechanical properties for steel fuse

4.3 Analytical Model Description and Building Resistance

The computed response in the specimens was obtained with the computer program for a two-dimensional nonlinear dynamic analysis, Ruaumoko [12]. The results were compared with those obtained experimentally to determine whether the analytical model could be used for later parametric studies. Because of the symmetry of the building, a two-dimensional analysis was chosen instead of a three-dimensional analysis, since the response of the transversal framework and behavior outside the plane of the elements was considered negligible. 68 nodes and 27 flexural elements were used. A detailed description of the analytical model and the mechanical properties of the elements are shown in [11]. The hysteresis rule for the analytical model was based on degradation of rigidity and strength. It was necessary to evaluate the effective flexural stiffness, K_θ, the rotation at the start of strain hardening, θ_{sh}, and the ultimate rotation, θ_u, as well as M_p and M_u, calculated moments at fully plasticized section and the moment resisting section, respectively [13].

In order to determine the lateral strength of each building, a nonlinear static analysis with incremental loads and a triangular distribution was performed. From this analysis were obtained the seismic coefficient V_b/W and the roof drift ratio D_r, defined as the ratio of the displacement of the last level of the building and its height relative to the base. Values for different seismic coefficients at different levels of seismic response were compared with the building seismic coefficient design, c_{DES}. The coefficients were: 1) the c_y coefficient, which indicates the building yielding point, where the building starts its inelastic behavior when one of the fuses reaches the value of the plastic moment, M_p, and 2) the value of the seismic coefficient, c_u, which corresponds to the maximum deflection capacity and it is defined for a roof drift ratio, D_r, equal to 0.05. The values of c_{DES}, c_y and c_u for the *EM1* building were 0.09, 0.12, 0.24, respectively, and for the *EM2* building, 0.22, 0.28, 0.61, respectively.

4.4 Ambient and Forced Vibration tests

These tests were performed to obtain the elastic frequencies and the fraction of critical damping of the test units, and to obtain some parameters' values for the analytical model. The lateral load on the forced vibration test was applied at the roof level and corresponded to a value of 500 N, associated with 6% and 3% of the basal shear design for the *EM1* and *EM2* buildings, respectively. The logarithmic decrement method was used to estimate the critical damping fraction, ξ, and the first mode of vibration period of the structure [14]. The results of the measurements were a fundamental period *T* equal to 0.67sec and 0.45sec for the *EM1* and *EM2* buildings, respectively, and a fraction of critical damping equal to 1.6 % and 1.8% for the *EM1* and *EM2* buildings, respectively.

4.5 Earthquakes tests

Ground motions recorded in Llolleo station, during the March 3rth of 1985 Chile Earthquake was selected to perform the test because it had a response spectrum similar to the design spectrum for the coast of Acapulco, Guerrero, *DII* zone, defined by [15]. Also, the record had small displacements, which was convenient considering the limitations of displacements of the shaking table. This record was selected because in Mexico there were not ground motion records with the mentioned characteristics. Fig. 4a shows the Llolleo record, and the value of maximum acceleration recorded. Fig. 4b compares the design spectrum for 5% of damping specified in the code (white diamonds and identified as *Z-DII*), with the elastic response spectrum for the selected earthquake (continue thick line identified as $\mu=1$). Additionally, this figure shows different inelastic response spectra calculated for some displacement ductility, μ. This figure shows two points related to the first building mode and the maximum deformation capacity, c_u, from a nonlinear static analysis. As shown in this figure, those points, circles and triangles, for the buildings *EM1* and *EM2*, respectively, are close to the spectral curves with ductility, μ, of 3 and 4. This means that the structures would have an important inelastic behavior during the test.

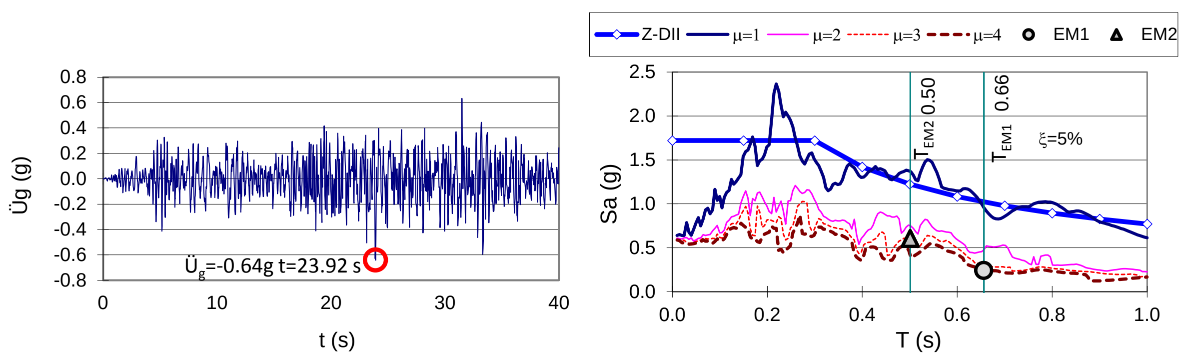

a) Accelerogram b) Response Spectra

Fig. 4. Signal characteristics and response spectra

4.6.2 Low Intensity Earthquake test

This test was carried out to 1) obtain measurements of the elastic response of the structure, 2) verify the dynamic properties of the structures obtained in the ambient and forced vibration tests conducted using low intensity signals and 3) verify that the accelerometers and displacement transducers worked properly. To achieve these objectives, the ordinates of the record shown in Fig. 4a were affected by the 0.1 factor.

A signal analysis with the transfer function between the target signal and the acceleration in the base of the structure during the test showed that the relationship in amplitude is different to one in frequencies above 15 Hz, due to the noise of the shaking table. This shows that the first three vibration modes were not distorted at the shaking table tests because the theoretical frequencies for the third mode were 12.5 and 15 Hz for the buildings EM1 and EM2, respectively, [11]

4.6.3 High Intensity Earthquake test

This is the last test performed in the *EM1* and *EM2* test units in order to study their inelastic behavior.

A signal analysis with the transfer function of the target signal and the acceleration in the base of the structure during the test showed that the amplitude ratio varies around the value of 1 in most of the frequencies, so it follows that the noise of the shaking table did not distort the vibration modes. However, to be consistent with the results obtained in the low-intensity earthquake, only frequencies less than 15 Hz were considered for the analysis of the building response [11].

4.6.4 Identification of Dynamic Properties

The fundamental vibration periods and modal shapes for the low intensity tests were identified with the transfer functions between the measured absolute accelerations at each level of the building and the recorded accelerations of the input motion. They were compared with those obtained with the Ruaumoko program and the results of the forced vibration test. The comparison of experimental and analytical results showed a good correlation [11].

4.6.5 Comparison of experimental and analytical results

In the following, a comparison is made of the envelopes of displacement and acceleration values of experimental and analytical results for the high intensity test, Fig 5. Analytical results were obtained from nonlinear dynamic analysis using the recorded input motion at the base and considering *P-Delta* effect. Fig 5 shows that results of the analytical model and experimental results have an acceptable correlation [11].

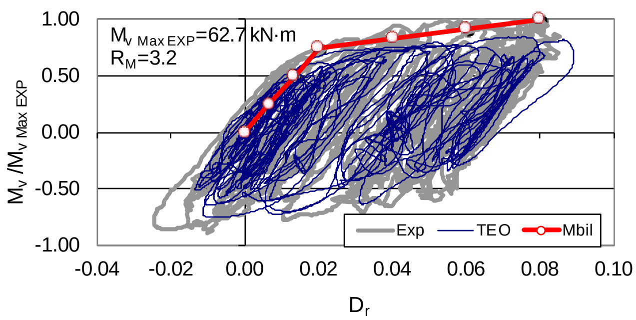

a) EM1

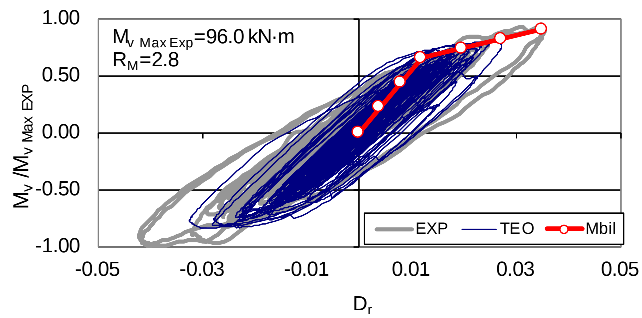

b) EM2

Fig. 5. Distortion vs overturning moment for the evaluation of inelastic behavior o

Fig. 5 compares the experimental hysteretic cycles (Exp) and analytical hysteretic cycles (Teo) overturning moment, M_v, versus roof drift ratio, D_r. To compare dimensionless parameters, the overturning moment is divided by the maximum value of overturning moment, $M_{v\ max\ EXP}$, calculated with the experimental accelerations. Fig. 5a shows the EM1 building hysteretic cycles are non-symmetrical with the vertical axis, this is because after 22s, the structure underwent major inelastic incursions. Fig. 5b for the EM2 building shows symmetrical cycles and also shows that the structure had important inelastic incursions. In order to evaluate the overall displacement ductility of the buildings, a bilinear curve envelope of the hysteretic cycles (M_{bil} in Fig. 5) was obtained. Based on the roof drift ratio envelope for the building EM1 (Fig. 5a), the values of roof drift ratio at yielding and ultimate levels were 0.02 to 0.08, respectively. The ratio of these values indicates that the building reached a global displacement ductility factor, μ, of 4. With the same procedure for building EM2, roof drift ratios at yielding and ultimate levels were 0.012 and 0.035, respectively (Fig. 5b), and a value of global displacement ductility of 2.9 was obtained.

Fig. 5 also shows values of the reduction factor R_M, defined above, and it was obtained from the analysis of the inelastic behavior of the buildings. It can be seen that the structures in all cases showed a relevant inelastic behavior as values of the R_M parameter were close to 3. In both structures, the value of the seismic coefficient obtained from experimental results, c_{MAX}, is close to the maximum value, c_u, computed from a push-over analysis. The experimental value of c_{MAX}, were 0.2 and 0.55 for the *EM1* and *EM2* buildings, respectively. It can be inferred that the test units suffered considerable damage.

4.6.6 Evaluation of horizontal floor accelerations during High Intensity tests

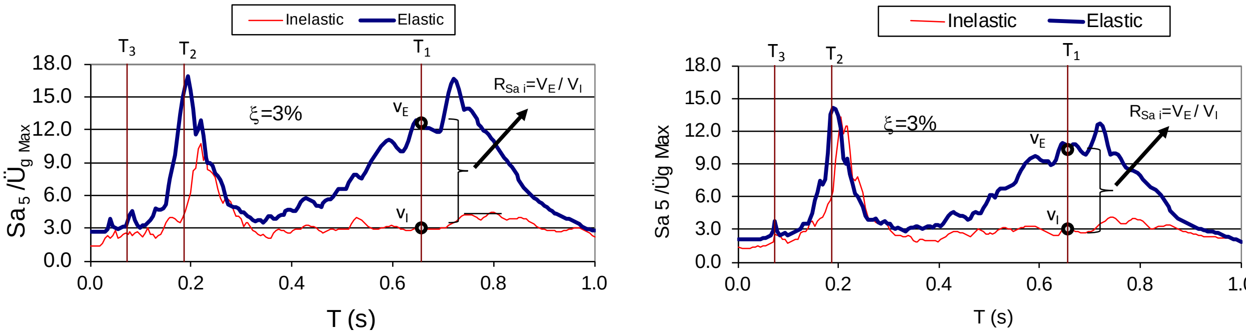

a) Experimental b) Calculated

Fig. 6. Spectra floor of the last level for the EM1 building for earthquake of low intensity and high intensity tests

One objective of this research was to study the response of floor accelerations in a building subjected to seismic excitation. Fig. 6 illustrates the horizontal floor acceleration spectra for the EM1 building. The thick line represents the elastic dimensionless acceleration spectra; measured at the roof level in the low intensity test, and the thin line shows the dimensionless acceleration spectra at the roof level in the high level test. The values of the ordinates in these spectra are dimensionless ratios of the measured horizontal floor acceleration and the maximum ground acceleration, $\grave{U}_{g\ max}$. A similar procedure was followed for the EM2 building [11]. Fig. 6 also shows the variation of the reduction factor for the mode *i*, R_{sai}. This parameter is calculated for each vibration period, considering the case where the structure is elastic and the case in which it suffers damage due to earthquake. R_{sai} is defined as the ratio of the value in the elastic accelerations spectrum and the value in the inelastic accelerations spectrum. These figures clearly show that the largest reductions due to inelastic behavior corresponds to the first mode, with values close to three. For modes 2 and 3, these reductions are small and vary between one and two, Fig. 6.

5. FORCES ANALYSIS

A study of measured horizontal floor accelerations in shaking-table tests [7] confirm the validity of the criteria for evaluating the floor forces in the last level proposed in [6] and applied in Eq. (4) to (6).

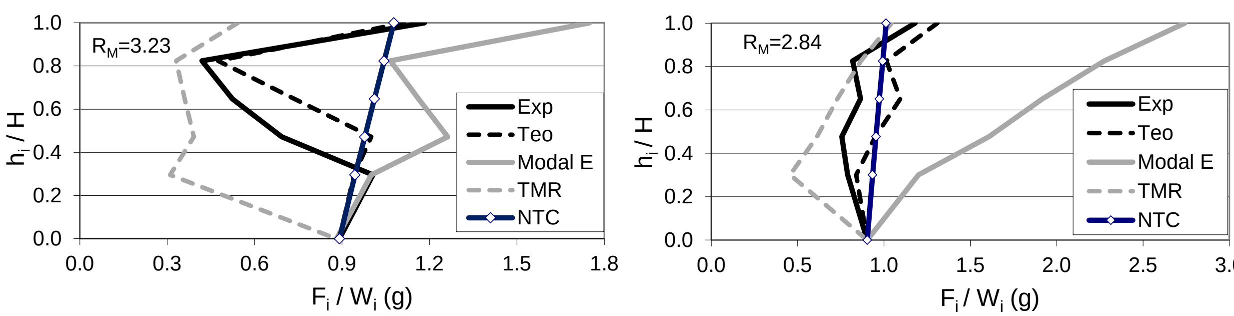

a) Building EM1 b) Building EM2

Fig. 7 Predicted and measured horizontal floor accelerations

Fig. 7 compares the envelope of forces obtained in the high intensity test (black solid line and identified as *Exp*), the envelope obtained from the theoretical model described above using the computer program for the nonlinear dynamic analysis, Ruaumoko, [12] (black dashed line and identified as *Teo*), and the envelopes for floor forces evaluated with different procedures. One of them is the envelope of the elastic forces and it is obtained with the modal superposition of the square root of the sum of squares of the accelerations (gray solid line and identifies as *Modal E*), the other one is the envelope of the floor forces when the contribution of all modes is reduced by the R_M factor (gray dotted line and identified as *TMR*) and third one is the envelope of the floor forces evaluated with the expression for diaphragms specified in [4] (thick continue line with white diamonds mark and identified as *NTC*). The results of these analytical studies were compared with the results obtained experimentally to determine whether the former could be used to meet the objectives proposed in this research.

As shown in these graphs, reducing all modes by a single value, that is, to divide the two terms of Eq. (4) by R_M, underestimates significantly the values of the floor forces. The use of the elastic modal response, considering R_M equal to 1 in Eq. (4), overestimates the floor acceleration response at all levels. These two curves, *Modal E* and *TMR*, presented great dispersion in predicting the inertial forces at all levels. The procedure specified by the [4], shown as *NTC* in Fig 7, also has a significant dispersion, mainly for the *EM1* building. The main drawback of this expression is that it does not represent an appropriated physical model, nor have a good correlation with results of other analyzes [7], [8] and [6].

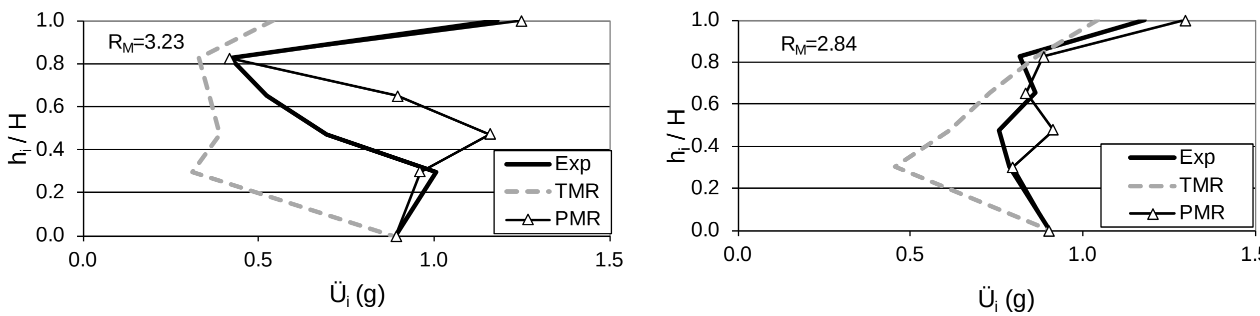

a) Building EM1 b) Building EM2

Fig. 8. Measured and predicted horizontal floor accelerations using TMR and PMR procedures

Fig. 8 shows again the envelope of forces *TMR*, which reduces the contribution of all modes by inelastic behavior, the envelope of experimental forces *Exp*, and compared with the envelope of forces using the first mode reduced procedure, specified in Eq. (4) (black thin line with white triangles and identified as *PMR*). The *PMR* approach for the evaluation of the floor force at all levels is based on reducing only the contribution of the first mode by nonlinear behavior in. As seen in this figure, the *PMR* procedure seems appropriated for the computation of earthquake horizontal floor accelerations when a structure has inelastic behavior. Furthermore, the PMR procedure is simple, and leads to an acceptable prediction of forces at all levels. It must be emphasized that the criterion of affecting the contribution of all modes due to inelastic behavior, largely underestimates the value of the inertial forces, which means that the designed structure might be unsafe.

Fig. 9 compares an envelope of measured horizontal floor accelerations along the building height, with envelopes of horizontal floor accelerations using two proposals [8]. The first is the code change proposal for diaphragm seismic design for the MCBC, and is given by Eq. (6) (dotted line and identified as *Rod–Res NTSC*). The second code proposal corresponds to the standard ASCE 7-16, given by Eq. (10)). The parameter R_s was assumed equal to 1 (solid gray line and identified as *ASCE 7-16*), with Z_s, equal to 0.7, and the contributing factors of the first mode and higher modes, Γ_{m1} and Γ_{m2}, equal to 1.28 and 0.85, respectively. The seismic coefficient for the higher modes, C_{s2}, was assumed equal to 0.89. The over strength factor, Ω_0, was obtained from the ratio of coefficients c_u and c_y, and was equal to 2.0 for *EM*1, and equal to 2.2 for the *EM2* building. The value of the seismic coefficient for the first mode, C_s, was equal to 0.28 and 0.34 for the *EM1* and *EM2* buildings, respectively. The modification factor for inelastic behavior, *R*, was taken equal to the ratio of the elastic an inelastic overturning moments, R_M, calculated for each building. The results show that the proposed procedures for estimating the design horizontal floor accelerations lead to results that have an acceptable correlation with the experimental results found in this investigation.

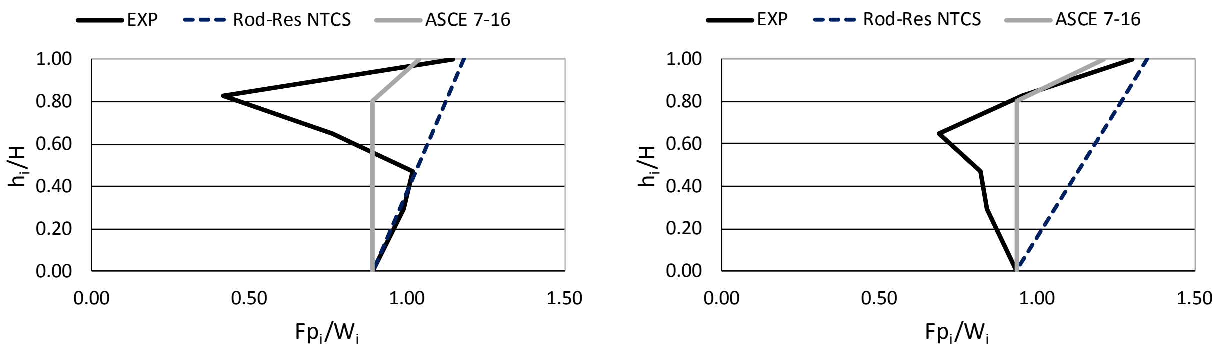

a) Building EM1 b) Building EM2

Fig. 9 Code predictions and measured horizontal floor accelerations

6. CONCLUSIONS

The following conclusions were obtained from this study.

1. The floor systems in buildings must transfer the horizontal inertial forces caused by earthquakes to vertical seismic resistant elements. It is recommended that this transfer of forces takes place without damage to the floor system, i.e., the earthquake energy dissipation is mainly present in the elements designed for this purpose, such as beams, walls, and columns.

2. The results of this study are consistent with previous studies, and show that reduction of horizontal floor forces is due to mainly the inelastic response of the first mode of vibration of the structure. The contribution of the higher modes is mainly elastic during the inelastic building response.

3. It was found that provisions of the current Mexican Code, and some state codes, to evaluate the in-plane design force for floor systems in buildings may lead to unsafe designs.

4. A procedure is proposed to define the horizontal inertial forces in rigid diaphragms. Comparison of results of test units of this study applying this procedure and those obtained experimentally, as well as results from time-history analysis showed an acceptable correlation.

7. Acknowledgements

This research was supported by the Institute of Engineering (UNAM) and CONACYT (Project 1085PA). Thanks are due to Professor Jose I. Restrepo of the University of California, San Diego, for his interest and time spent on this research, and for providing useful information for the design of the test units tested in this study.

8. References

[1] Hall, J. (1995) Northridge Earthquake of January 17. 1994 Reconnaissance Report. Vol.1. Earthquake Spectra. Supplement C to Volume 11. Publication 95-03

[2] Fleischman, R., Sause, R., Pessiki, S. y Rhodes, A. (1998) Seismic Behavior of Precast Parking Structure Diaphragms. PCI Journal. enero-febrero

[3] Priestley, M., Sritharan, S., Conley, J. y Pampanin, S. (1999) Preliminary Results and Conclusions from the PRESS Four-Story Precast Concrete Test Building PCI Journal. noviembre-diciembre

[4] NTCDC (2004) Normas Técnicas Complementarias para Diseño y Construcción de Estructuras de Concreto del Reglamento de Construcciones del Distrito Federal. Gaceta Oficial del Departamento del Distrito Federal. México DF

[5] ASCE 7-10. American Society of Civil Engineers. Minimum Design Loads for Buildings and Other Structures. Structural Engineering Institute. USA. 2010

[6] Rodriguez, M., Restrepo, J. y Carr, A. (2002) Earthquake induced floor horizontal accelerations in buildings. Earthquake Engineering - Structural Dynamics. 31. pp 693-718

[7] Rodriguez, M., Restrepo, J. y Blandón, J. (2007) Seismic Design Forces for Rigid Floor Diaphragms in Precast Concrete Building Structures. Journal of Structural Engineering. ASCE. November 2007. 1604-1615

[8] Rodriguez, M. y Restrepo, J. (2012). Práctica y Diseño Sísmico de Edificios en México -Cambios Necesarios. Revista de Ingeniería Sísmica No. 86 89-118 (2012)

[9] ASCE 7-16. (2017) American Society of Civil Engineers. Minimum Design Loads for Buildings and Other Structures. Structural Engineering Institute. USA. To be released in 2017.

[10] Kao, G. (1998) Design and Shake-Table Tests of a Four-Story Miniature Structure Built with Replaceable Plastic Hinges. M.E. Thesis. Department of Civil Engineering. University of Canterbury. Christchurch

[11] Blandon J y Rodríguez M. Estudio analítico-experimental y propuesta de diseño sísmico de sistema de pisos rígidos en edificios. Serie Investigación y Desarrollo. Instituto de Ingeniería UNAM. SID 656. Septiembre 2007

[12] Carr, A. (2003) RUAUMOKO. Computer Program Library. University of Canterbury. Department of Civil Engineering

[13] Dodd, L, y Restrepo, J (1995), Model for predicting cyclic behavior of reinforcing steel, Journal of Structural Engineering, 121(3), mar, 433-445

[14] Clough, A. y Penzien. J. (1993) Dynamics of Structures. Segunda edición. Mc Graw Hill. U.S.A

[15] NTCDS-EG (1993) Normas Técnicas Complementarias para Diseño por Sismo del Reglamento de Construcciones del Estado de Guerrero. F